Mechanics of Advanced Composite Structures 2 (2015) 79-93

Semnan University

Mechanics of Advanced Composite Structures

journal homepage: http://macs.journals.semnan.ac.ir

Free Vibrations Analysis of Functionally Graded Rectangular Nano-plates based on Nonlocal Exponential Shear Deformation Theory

K. Khorshidi*, T. Asgari, A. Fallah

Department of Mechanical Engineering, Faculty of Engineering, Arak, Iran

PAPER INFO

Paper history:
Received 24 September 2015
Received in revised form 6 November 2015
Accepted 22 November 2015

Keywords:
Vibration
Functionally graded nanoplates
Nonlocal elasticity
Exponential shear deformation theory

ABSTRACT

In the present study the free vibration analysis of the functionally graded rectangular nanoplates is investigated. The nonlocal elasticity theory based on the exponential shear deformation theory has been used to obtain the natural frequencies of the nanoplate. In exponential shear deformation theory an exponential functions are used in terms of thickness coordinate to include the effect of transverse shear deformation and rotary inertia. The nonlocal elasticity theory is employed to investigate the effect of the small scale on the natural frequency of the functionally graded rectangular nanoplate. The govering equations and the corresponding boundary conditions are derived by implementing Hamilton's principle. To show the accuracy of the formulations, the present results in specific cases are compared with available results in the literature and a good agreement is seen. Finally, the effect of the various parameters such as the nonlocal parameter, the power law indexes, the aspect ratio η , *and the thickness to lenghth ratio* δ on the natural frequencies of the rectangular FG nanoplates is presented and discussed in detail.

1. Introduction

The invention of carbon nanotubes (CNTs) initiated a new era in the nano world [1]. Since then, many studies have been performed in the field of the mechanical, electrical, physical and chemical behaviors of the nanostructures. The primary studies show that the mechanical properties of the nanostructures are different from other well-known materials [2]. The superior properties of these structures have led to their applications in many fields such as nanodevices, nanooscillators, nanobearings, hydrogen storage, and electrical batteries. The plate-like nanostructures such as nanoplates or nano-scale sheets are very important types of the nanostructures with two-dimensional shapes. They possess extraordinary mechanical properties[1-6] and these unique properties make them ideal candidates for multifarious field of nanotechnology industry including energy storage[7], nano electromechanical systems [8], strain, mass and pressure sensors [9, 10], solar cells [11], photo-catalytic degradation of organic dye [12], composite materials [13] and ect. The continuum modeling of the nanomaterials has received a great deal of attention of the scientific community because the controlled experiments in nanoscale are difficult and molecular dynamic simulations are highly expensive computationally. There are various size dependent continuum theories such as couple stress theory [14], strain gradient elasticity theory [15], modified couple stress theory [16] and nonlocal elasticity theory [17]. Among these theories, the nonlocal elasticity theory has been widely applied [18-24]. To overcome the shortcomings of the classical elasticity theory, Eringen and Edelen[17] introduced the nonlocal elasticity theory in 1972. They modified the

*Corresponding author, Tel.: +98-863-2625050; fax: +98-863-4173450

E-mail address: k-khorshidi@araku.ac.ir

classical continuum mechanics for taking into account the small scale effects. According to the nonlocal elasticity theory, the stress tensor at an arbitrary point in the domain of nanomaterial depends not only on the strain tensor at that point but also on the strain tensor at all other points in the domain. Both the atomistic simulation results and the experimental observations on phonon dispersion have shown the accuracy of this observation [25, 26]. The Functionally Graded Materials (FGMs) are the new generation of novel composite materials in the family of engineering composites, whose properties are varied smoothly in the spatial direction microscopically to improve the overall structural performance. These materials offer a great promise in high temperature environments, for example, wear-resistant linings for handling large heavy abrasive ore particles, rocket heat shields, heat exchanger tubes, thermo-electric generators, heat heat engine components, plasma facings for fusion reactors, and electrically insulating metal/ceramic joints, and also these are widely used in many structural applications such as mechanics, civil engineering, optical, electronic, chemical, biomedical, energy sources, nuclear, automotive fields, and ship building industries to minimize the thermomechanical mismatch in metal-ceramic bonding. Most structures, irrespective of their use, are subjected to dynamic loads during their operational life. Increased use of nano-FGMs in various structures such as thermo-nanoactuators, thermo-nanosensors, thermao-pressure sensors andetcapplications necessitates the development of accurate theoretical models to predict their response.In past decades, the free vibration of functionally graded materials has been studied extensively. Malekzadeh and Heydarpour [27] investigated the free vibration analysis of rotating functionally graded cylindrical shells subjected to thermal environment based on the First-order Shear Deformation Theory (FSDT) of shells. The formulation included the centrifugal and coriolis forces due to the rotation of the shell. The differential quadrature method was adopted to discretise the thermoelastic equilibrium equations and the equations of motion. Ungbhakorn and wattanasakulpong[28]presented thermo-elastic vibration response of functionally graded plates carring distributed patch mass based on third-order shear deformation theory. The solutions were obtained using the energy method. In addition, the forced vibration analysis with external dynamic load acting on the sub-domain of the patch mass was also discussed. Kumar and Lal [29] predicted the first three natural frequencies of the free axisymmetric vibration of the two-directional functionally graded annulr plates resting upon winkler foundation using differential quadrature method and Chabyshev collocation technique. Frequency equations for a plate clamped at both the edges and another plate simply supported at both the edges were obtained. Based on the three-dimensional theory of elasticity and assuming that the mechanical properties of the materials varied continuously in the thickness direction and had the same exponent-law variations, the three-dimensional free and forced vibration analysis of functionally graded circular plate with various boundary conditions was achieved by Nie and Zhong[30]. Hung et al [31] investigated the free vibrations of rectangular FGM plates through internal cracks using the Ritz method. Three-dimensional elasticity theory was employed, and new sets of admissible functions for the displacement fields were proposed to enhance the effectiveness of the Ritz method in modelling the behaviors of the cracked plates. Matsunaga [32] analysed the natural frequencies and buckling stresses of plates made of functionally graded materials by taking into account the effects of transverse shear and normal deformations and rotatory inertia. By using the method of power series expansion of displacement components, a set of functionally graded (FG) plates was derived using Hamilton's principle. Malekzadeh and Alibeygi[33] presented the free vibration of functionally graded arbitrary straight-sided quadrilateral plates under the thermal environment and based on the first-order shear deformation theory. The differential quadrature method was adopted to discretise the equilibrium equations. The free vibration of functionally graded micro/nano plates was also considered in recent years.Ke et al [34] developed a non-classical microplate model for the axisymmetric nonlinear free vibration analysis of annular microplates made of functionally graded materials based on the modified couple stress theory, Mindlin plate theory and von-Karman geometric nonlinearity theory. The non-classical model was capable of shear deformation and rotary inertia.Ke et al [35] also studied the bendig, buckling and free vibration of annular microplates made of functionally graded materials based on the modified couple stress theory and Mindlin plate theory. The material properties of the FGM microplates were assumed to vary in the thickness direction and were estimated using the Mori-Tanaka homogenization technique. Asghari and Taati[36] presented a size-dependent formulation for mechanical analyses of inhomogeneous micro-plates based on the modified couple stress theory. The govering differential equations of the motion were derived for functionally graded plates with arbitrary shapes utilizing a variational approach. Utilizing the derived formulation, the free-vibration behaviour as well as the static re-

sponse of a rectangular FG micro-plate was proposed. Nataraja et al [37] investigated the size-dependent linear free flexural vibration behaviour of functionally graded nanoplates using the iso-geometric based finite element method. The field variables were approximated by non-uniform rational B-splines. The nonlocal constitutive relation was based on the Eringen's differential form of the nonlocal elasticity theory.

In the present study, as a first endeavor, the free vibration of functionally graded nanoplates is investigated based on the exponential shear deformation theory and using the nonlocal elasticity theory. The Navier solution is used to study the free vibration of the functionally graded nanoplates. It is assumed that the material properties are varying through the thickness according to the power law distribution. The results of the present work may be used as bench marks for future studies.

2. Theoretical formulations

Consider a rectangular nanoplate of length a, width b, and total thickness h and composed of functionally graded materials through the thickness as shown in Figure 1. The properties of the nanoplate are assumed to vary through the thickness of the nanoplate with a power-law distribution of the volume fractions of the two materials between the two surfaces. In fact, the top surface ($z = h/2$) of the nanoplate is ceramic-rich whereas the bottom surface ($z = -h/2$) is metal-rich.

Young's modulus and mass density are assumed to vary continuously through the thickness as what follows [38]

$$E(z) = (E_c - E_m)V_f(z) + E_m \quad (1)$$

$$\rho(z) = (\rho_c - \rho_m)V_f(z) + \rho_m \quad (2)$$

where the subscripts m and c represent the metallic and ceramic constituents, respectively, and $V_f(z)$ is the volume fraction that may be given by the following equation:

$$V_f(z) = \left(\frac{z}{h} + \frac{1}{2}\right)^g \quad (3)$$

where g is the power-law index and takes only posetive values. Poisson's ratio υ is the same for all the metal/ceramic materials that are used here, so it is assumed to be constant and is taken to be 0.3 throughout the analysis[39]. The typical values for metals and ceramics used in the FG nanoplate are listed in Table 1.

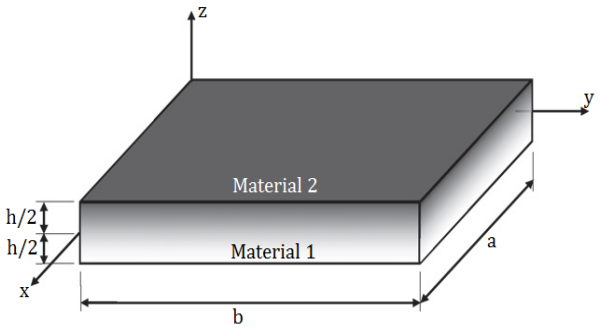

Figure 1. The geometry of a FGM plate

Table 1. The material properties of the used FG plate

Material	Properties		
	E (GPa)	υ	$\rho(kg/m^3)$
Aluminum (Al)	70	0.3	2702
Alumina (Al_2o_3)	380	0.3	3800
Zirconia (ZrO_2)	200	0.3	5700

2.1. The nonlocal elasticity theory

In nonlocal theory stress field at each body point body is a function of the strain field. So stress plays a major role in the theory which is defined as what follows [40]:

$$t_{ij} = \int_V \alpha(|X' - X|)\sigma_{ij}(X')dV' \quad (4)$$

where X is a point on the body that the stress tensor on its efficacy, X' can be any point else in the body, $V$is the volume of a region of the body that integral is taken on it,σ_{ij} is the local stress tensor, $\alpha(|X' - X|)$ is the nonlocal kernel function related to the internal characteristic length. With respect to properties of nonlocal kernel function $\alpha(|X' - X|)$ that are discussed by Eringen[41], taking in a Greens function of a linear differential operator, $\mathcal{L}$, can be defined as following,

$$\mathcal{L}\alpha(|X' - X|) = \delta\alpha(|X' - X|), \quad (5)$$

Substituting Eq. (5) into Eq. (4), the primary relation (1) form of the following differential equation is obtained as

$$\mathcal{L}t_{ij} = \sigma_{ij}, \quad (6)$$

For the nonlocal linear elastic solids, the equations of motion have the following form [42]:

$$t_{ij,j} + f_i = \rho(z)\ddot{u}_i, \quad (7)$$

Where ρ is the mass density, f_i body forces and u_i is the displacement vector. Substituting Eq. (7) into Eq. (6) yields to what follows:

$$\sigma_{ij} + \mathcal{L}(f_i - \rho(z)\ddot{u}_i) = 0, \quad (8)$$

The nonlocal model with the linear differential operator $\mathcal{L}$ for the two-dimensional case is defined by the following equation [9]:

$$\mathcal{L} = 1 - \mu^2\nabla^2, \quad (9)$$

where ∇^2 is the Laplace operator, which in cartesian coordinates is $\nabla^2 = \partial^2/\partial x^2 + \partial^2/\partial y^2$ and $\mu = e_0 a, a$ is the internal characteristic length and e_0 is the material constant which is specified by the experiment. The value of the small-scale parameter is dependent on the boundary condition, the chirality, the mode shapes, the number of walls, and the nature of motions [43]. There is no accurate way to calculate this factor, but it is suggested that the coefficient be determined by conducting a comparison of dispersion curves from nonlocal continuum mechanics and lattice dynamics of nano-material crystal structure [43].

2.2. The assumptions made in the proposed theory

1. The displacement components u and v are the in-plane displacements of the middle surface in x and y directions respectively, and w is the deflection of the middle surface in z direction. The magnitude of the deflection w is not of the same order as the thickness h of the plate and is small with respect to the plate thickness.

2. The in-plane displacements, u and v, include three parts:

a) A displacement component equivalent to the displacement in the classical plate theory.

b) A displacement component owing to the shear deformation which is assumed to be harmonic in nature with respect to the thickness coordinate.

c) The shear strains in z direction are zero in the top and bottom surfaces of the plates.

3. The deflection w in z direction is assumed to be a function of x and y coordinates.

4. The plate is subjected to the transverse load only.

The displacement field of the exponential shear deformation theory is given as below [44]:

$$u(x,y,z,t) = u_0(x,y,z,t) - z\frac{\partial w(x,y,t)}{\partial x} + f(z)\phi(x,y,t), \quad (10a)$$

$$v(x,y,z,t) = v_0(x,y,z,t) - z\frac{\partial w(x,y,t)}{\partial y} + f(z)\psi(x,y,t), \quad (10b)$$

$$W(x,y,z,t) = w(x,y,t), \quad (10c)$$

Where $f(z) = z\left(e^{-2\left(\frac{z}{h}\right)^2}\right)$ and u, v and w are displacements in the x, y and z directions respectively, and u_0 and v_0 are the mid-plane displacements and ϕ *and* ψ are the rotation functions. With the linear assumption of von-Karman strain, the displacement strain field will be as what follows:

$$\varepsilon_{ij} = \frac{1}{2}\left(u_{i,j} + u_{j,i}\right),\ i, j = x,y,z \quad (11)$$

Considering Hooke's Law for stress field, the normal stress σ_{zz} is assumed to be negligible in comparison with the plane stresses σ_{xx} and σ_{yy}.Thus stress-strain relationship will be as what follows:

$$\sigma_{xx} = \frac{E(z)}{1-\upsilon^2}\left(\varepsilon_{xx} + \nu\varepsilon_{yy}\right), \quad (12a)$$

$$\sigma_{yy} = \frac{E(z)}{1-\upsilon^2}\left(\varepsilon_{yy} + \nu\varepsilon_{xx}\right), \quad (12b)$$

$$\sigma_{xy} = 2G(z)\varepsilon_{xy}, \quad (12c)$$

$$\sigma_{xz} = 2G(z)\varepsilon_{xz}, \quad (12d)$$

$$\sigma_{yz} = 2G(z)\varepsilon_{yz}, \quad (12e)$$

Substuting Eqs. (11) into Eq. (12), the displacement stress field will be as what follows:

$$\begin{Bmatrix} \sigma_{xx} \\ \sigma_{yy} \\ \sigma_{xy} \\ \sigma_{xz} \\ \sigma_{yx} \end{Bmatrix} = \frac{E(z)}{1-\nu^2} \left(\begin{Bmatrix} f(z)\left(\frac{\partial\varphi}{\partial x} + \upsilon\frac{\partial\psi}{\partial y}\right) \\ f(z)\left(\frac{\partial\psi}{\partial y} + \upsilon\frac{\partial\varphi}{\partial x}\right) \\ \left(\frac{1-\upsilon}{2}\right) f(z)\left(\frac{\partial\varphi}{\partial y} + \upsilon\frac{\partial\psi}{\partial x}\right) \\ \left(\frac{1-\upsilon}{2}\right)\frac{df(z)}{dz}\varphi \\ \left(\frac{1-\upsilon}{2}\right)\frac{df(z)}{dz}\psi \end{Bmatrix} \begin{Bmatrix} \frac{\partial u_0}{\partial x} + \upsilon\frac{\partial v_0}{\partial y} \\ \frac{\partial v_0}{\partial y} + \upsilon\frac{\partial u_0}{\partial x} \\ \frac{(1-\upsilon)}{2}\left(\frac{\partial u_0}{\partial y} + \upsilon\frac{\partial v_0}{\partial x}\right) \\ \frac{(1-\upsilon)}{2}\frac{\partial u_0}{\partial z} \\ \frac{(1-\upsilon)}{2}\frac{\partial v_0}{\partial z} \end{Bmatrix} - z\begin{Bmatrix} \frac{\partial^2 w}{\partial x^2} + \upsilon\frac{\partial^2 w}{\partial y^2} \\ \frac{\partial^2 w}{\partial y^2} + \upsilon\frac{\partial^2 w}{\partial x^2} \\ (1-\upsilon)\frac{\partial^2 w}{\partial x\partial y} \\ 0 \\ 0 \end{Bmatrix} \right) \quad (13)$$

Using Eq. (6) the stress-displacement constitutive relation of a nonlocal FG plate can be written as:

$$(1-\mu\nabla^2)\begin{Bmatrix}\sigma_{xx}^{NL}\\ \sigma_{yy}^{NL}\\ \sigma_{xy}^{NL}\\ \sigma_{xz}^{NL}\\ \sigma_{yz}^{NL}\end{Bmatrix}=-\frac{E(z)}{1-\nu^2}z\begin{Bmatrix}\frac{\partial^2 w}{\partial x^2}+\upsilon\frac{\partial^2 w}{\partial y^2}\\ \frac{\partial^2 w}{\partial y^2}+\upsilon\frac{\partial^2 w}{\partial x^2}\\ (1-\upsilon)\frac{\partial^2 w}{\partial x\partial y}\\ 0\\ 0\end{Bmatrix}+$$

$$\frac{E(z)}{1-\nu^2}\left(\begin{Bmatrix} f(z)\left(\frac{\partial\varphi}{\partial x}+\upsilon\frac{\partial\psi}{\partial y}\right)\\ f(z)\left(\frac{\partial\psi}{\partial y}+\upsilon\frac{\partial\varphi}{\partial x}\right)\\ \frac{1-\upsilon}{2}f(z)\left(\frac{\partial\varphi}{\partial y}+\upsilon\frac{\partial\psi}{\partial x}\right)\\ \frac{1-\upsilon}{2}\frac{df(z)}{dz}\varphi\\ \frac{1-\upsilon}{2}\frac{df(z)}{dz}\psi\end{Bmatrix}+\begin{Bmatrix}\frac{\partial u_0}{\partial x}+\upsilon\frac{\partial v_0}{\partial y}\\ \frac{\partial v_0}{\partial y}+\upsilon\frac{\partial u_0}{\partial x}\\ \frac{(1-\upsilon)}{2}\left(\frac{\partial u_0}{\partial y}+\upsilon\frac{\partial v_0}{\partial x}\right)\\ \frac{(1-\upsilon)}{2}\frac{\partial u_0}{\partial z}\\ \frac{(1-\upsilon)}{2}\frac{\partial v_0}{\partial y}\end{Bmatrix}\right) \tag{14}$$

where $E(z)$ is the Young's modulus, ν is the Poisson's ratio, and $G(z)=E(z)/2(1+\nu)$ is the shear modulus of the plate.

The Hamilton's principle is employed to extract the equation of motion. The Hamilton's principle in case of local form is obtained as what follows [44]:

$$\int_0^T(\delta U+\delta W-\delta T)dt=0, \tag{15}$$

where δ is the variation operator, U is the strain energy, W is the work done by external forces, and T is the kinetic energy.

$$\int_0^T\left(\int_{\frac{-h}{2}}^{\frac{h}{2}}\int_0^b\int_0^a(\sigma_{xx}\delta\varepsilon_{xx}+\sigma_{yy}\delta\varepsilon_{yy}+2\sigma_{xy}\delta\varepsilon_{xy}+2\sigma_{xz}\delta\varepsilon_{xz}+2\sigma_{yz}\delta\varepsilon_{yz})dxdydz-\frac{\delta}{2}\int_{\frac{-h}{2}}^{\frac{h}{2}}\int_0^b\int_0^a\rho(z)\left(\dot{u}^2+\dot{v}^2+\dot{w}^2\right)dxdydz\right)dt=0 \tag{16}$$

where the dot-top index contract indicates the differentiation with respect to the time variable. Exertion of variation operator on Eq. 16 should be as follows:

$$\delta\left(\frac{\partial i}{\partial j}\right)=\frac{\partial}{\partial j}\delta(i),\ i=\phi,\psi,\ j=x,y \tag{17a}$$

$$\delta\left(\frac{\partial^2 i}{\partial j\partial k}\right)=\frac{\partial^2}{\partial j\partial k}\delta(i),\ i=w,\ j=x,y,\ k=x,y \tag{17b}$$

$$\delta\left(\frac{\partial i}{\partial t}\right)^2=2\left(\frac{\partial i}{\partial t}\right)\frac{\partial}{\partial t}\delta(i),\ i=u,v,w \tag{17c}$$

Using Eqs. (17a)-(17c) and substituting Eq. (10) and (11) into Eq. (14), the following equations are obtained as follows,

$$\int_0^T\left(\int_{\frac{-h}{2}}^{\frac{h}{2}}\int_0^b\int_0^a\left[\sigma_{xx}\left(\frac{\partial}{\partial x}(\delta u_0)-z\frac{\partial^2}{\partial x^2}(\delta w)+f(z)\frac{\partial}{\partial x}(\delta\phi)\right)+\sigma_{yy}\left(\frac{\partial}{\partial x}(\delta v_0)-z\frac{\partial^2}{\partial y^2}(\delta w)+f(z)\frac{\partial}{\partial y}(\delta\psi)\right)\right.\right.$$
$$+\sigma_{xy}\left(-2z\frac{\partial^2}{\partial x\partial y}+f(z)\left(\frac{\partial}{\partial y}(\delta\phi)+\frac{\partial}{\partial x}(\delta\psi)\right)+\frac{\partial}{\partial y}(\delta u_0)+\frac{\partial}{\partial x}(\delta v_0)\right)$$
$$\left.\left.+\sigma_{xz}\left(\frac{\partial}{\partial z}(\delta u_0)+\frac{df(z)}{dz}\delta\phi\right)+\sigma_{yz}\left(\frac{\partial}{\partial z}(\delta u_0)+\frac{df(z)}{dz}\delta\psi\right)\right]dxdydz\right.$$
$$-\frac{1}{2}\int_{\frac{-h}{2}}^{\frac{h}{2}}\int_0^b\int_0^a\rho(z)\left[-2\frac{\partial^2 u_0}{\partial t^2}\delta u_0+2z\frac{\partial^3 u_0}{\partial t^3}\delta w+2z\left(\frac{\partial^3 w}{\partial x\partial t^2}\right)\delta u_0-2f(z)\frac{\partial^2 u_0}{\partial t^2}\delta\phi-\right.$$
$$2f(z)\frac{\partial^2\phi}{\partial t^2}\delta u_0-2\frac{\partial^2 v_0}{\partial t^2}\delta v_0+2z\frac{\partial^3 v_0}{\partial t^3}\delta w+2z\left(\frac{\partial^3 w}{\partial y\partial t^2}\right)\delta v_0-2f(z)\frac{\partial^2 v_0}{\partial t^2}\delta\psi-2f(z)\frac{\partial^2\psi}{\partial t^2}\delta v_0$$
$$+z^2\left(\frac{\partial^2 w}{\partial x\partial t}\right)\frac{\partial}{\partial x}-zf(z)\left(\frac{\partial^2 w}{\partial x\partial t}\right)\delta\phi-zf(z)\left(\frac{\partial\phi}{\partial t}\right)\frac{\partial}{\partial x}(\delta w)+(f(z))^2\left(\frac{\partial\phi}{\partial t}\right)\delta\phi$$
$$\left.+z^2\left(\frac{\partial^2 w}{\partial y\partial t}\right)\frac{\partial}{\partial y}(\delta w)-zf(z)\left(\frac{\partial^2 w}{\partial y\partial t}\right)\delta\psi\right.$$

$$-zf(z)\left(\frac{\partial\psi}{\partial t}\right)\frac{\partial}{\partial y}(\delta w)+$$
$$(f(z))^2\left(\frac{\partial\psi}{\partial t}\right)\delta\psi+w\delta w\Big]dxdydz\Big)dt \tag{18}$$

Using integration by parts and lemma of calculus of variations can be derived the equations of motion and boundary conditions from Eq. (16).

The relations between stress resultants in local and nonlocal theories can be find in Eq. (18), by calculating the coefficients of δu_0, δv_0, δw, $\delta\phi$, $\delta\psi$, in Eq. (16), the nonlocal equations of motion may be expressed as Eqs. (19a)–(19e).

$$\frac{\partial N_{xx}}{\partial x}+\frac{\partial N_{xy}}{\partial y}=I_0\frac{\partial^2 u_0}{\partial t^2}-I_1\frac{\partial^3 w}{\partial x\partial t^2}+I_3\frac{\partial^2\phi}{\partial t^2}$$
$$-\mu^2\Big(I_0\frac{\partial^4 u_0}{\partial t^2\partial x^2}-I_1\frac{\partial^5 w}{\partial y\partial t^2\partial x^2}+I_3\frac{\partial^4\phi}{\partial t^2\partial x^2}+$$
$$I_0\frac{\partial^4 u_0}{\partial t^2\partial y^2}-I_1\frac{\partial^5 w}{\partial x\partial t^2\partial y^2}+I_3\frac{\partial^4\phi}{\partial t^2\partial y^2}\Big) \tag{19a}$$

$$\frac{\partial N_{yy}}{\partial y}+\frac{\partial N_{xy}}{\partial x}=I_0\frac{\partial^2 v_0}{\partial t^2}-I_1\frac{\partial^3 w}{\partial y\partial t^2}+I_3\frac{\partial^2\psi}{\partial t^2}$$
$$-\mu^2\Big(I_0\frac{\partial^4 v_0}{\partial t^2\partial x^2}-I_1\frac{\partial^5 w}{\partial y\partial t^2\partial x^2}+I_3\frac{\partial^4\psi}{\partial t^2\partial x^2}+$$
$$I_0\frac{\partial^4 v_0}{\partial t^2\partial y^2}-I_1\frac{\partial^5 w}{\partial y\partial t^2\partial y^2}+I_3\frac{\partial^4\psi}{\partial t^2\partial y^2}\Big) \tag{19b}$$

$$\frac{\partial^2 M_{xx}}{\partial x^2}+2\frac{\partial^2 M_{xy}}{\partial x\partial y}+\frac{\partial^2 M_{yy}}{\partial y^2}=I_0\frac{\partial^2 w}{\partial t^2}+$$
$$I_1\Big(\frac{\partial^3 u_0}{\partial x\partial t^2}+\frac{\partial^3 v_0}{\partial y\partial t^2}\Big)-I_2\Big(\frac{\partial^4 w}{\partial x^2\partial t^2}+\frac{\partial^4 w}{\partial y^2\partial t^2}\Big)+$$
$$I_4\Big(\frac{\partial^4\phi}{\partial x\partial t^2}+\frac{\partial^4\psi}{\partial y\partial t^2}\Big)-\mu^2\Big(I_0\frac{\partial^4 w}{\partial t^2\partial x^2}+$$
$$I_1\Big(\frac{\partial^5 u_0}{\partial x\partial t^2\partial x^2}+\frac{\partial^5 v_0}{\partial y\partial t^2\partial x^2}\Big)-$$
$$I_2\Big(\frac{\partial^6 w}{\partial x^2\partial t^2\partial x^2}+\frac{\partial^6 w}{\partial y^2\partial t^2\partial x^2}\Big)$$
$$I_4\Big(\frac{\partial^5\phi}{\partial x\partial t^2\partial x^2}+\frac{\partial^5\psi}{\partial y\partial t^2\partial x^2}\Big)+I_0\frac{\partial^4 w}{\partial t^2\partial y^2}$$
$$I_1\Big(\frac{\partial^5 u_0}{\partial x\partial t^2\partial y^2}+\frac{\partial^5 v_0}{\partial y\partial t^2\partial y^2}\Big)-$$
$$I_2\Big(\frac{\partial^6 w}{\partial x^2\partial t^2\partial y^2}+\frac{\partial^6 w}{\partial y^2\partial t^2\partial y^2}\Big)+I_4\Big(\frac{\partial^4\phi}{\partial x\partial t^2\partial y^2}$$
$$+\frac{\partial^4\psi}{\partial y\partial t^2\partial y^2}\Big) \tag{19c}$$

$$\frac{\partial R_{xx}}{\partial y}+\frac{\partial R_{xy}}{\partial x}-Q_x=I_3\frac{\partial^2 u_0}{\partial t^2}-I_4\frac{\partial^3 w}{\partial x\partial t^2}+$$
$$I_5\frac{\partial^2\phi}{\partial t^2}-\mu^2\Big(I_3\frac{\partial^4 u_0}{\partial t^2\partial x^2}-I_4\frac{\partial^5 w}{\partial x\partial t^2\partial x^2}+$$
$$I_5\frac{\partial^4\phi}{\partial t^2\partial x^2}+I_3\frac{\partial^4 u_0}{\partial t^2\partial y^2}-I_4\frac{\partial^5 w}{\partial x\partial t^2\partial y^2}+$$
$$I_5\frac{\partial^4\phi}{\partial t^2\partial y^2}\Big) \tag{19d}$$

$$\frac{\partial R_{yy}}{\partial y}+\frac{\partial R_{xy}}{\partial x}-Q_y=I_3\frac{\partial^2 v_0}{\partial t^2}-I_4\frac{\partial^3 w}{\partial y\partial t^2}+$$
$$I_5\frac{\partial^2\psi}{\partial t^2}-\mu^2\Big(I_3\frac{\partial^4 v_0}{\partial t^2\partial x^2}-I_4\frac{\partial^5 w}{\partial y\partial t^2\partial x^2}+$$
$$I_5\frac{\partial^4\psi}{\partial t^2\partial x^2}+I_3\frac{\partial^4 v_0}{\partial t^2\partial y^2}-I_4\frac{\partial^5 w}{\partial y\partial t^2\partial y^2}+$$
$$I_5\frac{\partial^4\psi}{\partial t^2\partial y^2}\Big) \tag{19e}$$

where

$$\begin{cases}\left(1-\mu^2\nabla^2\right)R_i^{NL}=R_i^L, i=xx,yy,xy\\ \left(1-\mu^2\nabla^2\right)Q_i^{NL}=Q_i^L, i=x,y\\ \left(1-\mu^2\nabla^2\right)M_i^{NL}=M_i^L, i=xx,yy,xy\\ \left(1-\mu^2\nabla^2\right)N_i^{NL}=N_i^L, i=xx,yy,xy\end{cases} \tag{20a}$$

$$\left(I_0,I_1,I_2\right)=\int_{-\frac{h}{2}}^{\frac{h}{2}}\rho(1,z,z^2)dz, \tag{20b}$$

$$\left(I_3,I_4,I_5\right)=\int_{-\frac{h}{2}}^{\frac{h}{2}}\rho(z)\left(f(z),zf(z),(f(z))^2\right)dz, \tag{20c}$$

$$\left(R_{xx}^L,R_{yy}^L,R_{xy}^L\right)=\int_{-\frac{h}{2}}^{\frac{h}{2}}\left(\sigma_{xx},\sigma_{yy},\sigma_{xy}\right)f(z)dz, \tag{20d}$$

$$\left(Q_x^L,Q_y^L\right)=\int_{-\frac{h}{2}}^{\frac{h}{2}}\left(\sigma_{xz},\sigma_{yz}\right)\frac{df(z)}{dz}dz, \tag{20e}$$

$$\left(N_{xx}^L,N_{yy}^L,N_{xy}^L\right)=\int_{-\frac{h}{2}}^{\frac{h}{2}}\left(\sigma_{xx},\sigma_{yy},\sigma_{xy}\right)dz, \tag{20f}$$

$$\left(M_{xx}^L,M_{yy}^L,M_{xy}^L\right)=\int_{-\frac{h}{2}}^{\frac{h}{2}}\left(\sigma_{xx},\sigma_{yy},\sigma_{xy}\right)zdz, \tag{20g}$$

N and R are the force and M is the moment that is acting on the body. The following sets of boundary conditions at the edges of the plate are obtained as a result of the application of the Hamilton's principle:

Either $R_{xx}=0$ or ϕ prescribed at $x=0,a$
Either $R_{yy}=0$ or ψ prescribed at $y=0,b$ (21a)

Either $R_{xy}=0$ or ψ prescribed at $x=0,a$ Either $R_{xy}=0$ or ϕ prescribed at $y=0,b$ (21b)

Either $M_x=0$ or $\frac{\partial w}{\partial x}$ prescribed at $x=0,a$ (21c)

Either $M_y=0$ or $\frac{\partial w}{\partial y}$ prescribed at $y=0,b$

Either $\frac{\partial M_x}{\partial x}+2\frac{\partial M_{xy}}{\partial y}=0$ or w prescribed at $x=0,a$ (21d)

Either $\frac{\partial M_y}{\partial y}+2\frac{\partial M_{xy}}{\partial x}=0$ or prescribed at $y=0,b$

Either $N_x=0$ or at $x=0,a$ (21e)

Either $N_y=0$ or at $y=0,b$

Introducing the nonlocal stress resultants:

$$\begin{bmatrix} R_{xx} \\ R_{yy} \\ R_{xy} \end{bmatrix} = D\begin{bmatrix} \frac{\partial\phi}{\partial x}+\upsilon\frac{\partial\psi}{\partial y} \\ \frac{\partial\psi}{\partial y}+\upsilon\frac{\partial\phi}{\partial x} \\ \frac{1-\upsilon}{2}\left(\frac{\partial\phi}{\partial y}+\frac{\partial\psi}{\partial x}\right) \end{bmatrix} - A\begin{bmatrix} \frac{\partial^2 w}{\partial x^2}+\upsilon\frac{\partial^2 w}{\partial y^2} \\ \frac{\partial^2 w}{\partial y^2}+\upsilon\frac{\partial^2 w}{\partial x^2} \\ (1-\upsilon)\frac{\partial^2 w}{\partial x\partial y} \end{bmatrix} + C\begin{bmatrix} \frac{\partial u_0}{\partial x}+\upsilon\frac{\partial v_0}{\partial y} \\ \frac{\partial v_0}{\partial y}+\upsilon\frac{\partial u_0}{\partial x} \\ \frac{1-\upsilon}{2}\left(\frac{\partial u_0}{\partial y}+\frac{\partial v_0}{\partial x}\right) \end{bmatrix} \quad (22a)$$

$$\begin{bmatrix} M_{xx} \\ M_{yy} \\ M_{xy} \end{bmatrix} = A\begin{bmatrix} \frac{\partial\phi}{\partial x}+\upsilon\frac{\partial\psi}{\partial y} \\ \frac{\partial\psi}{\partial y}+\upsilon\frac{\partial\phi}{\partial x} \\ \frac{1-\upsilon}{2}\left(\frac{\partial\phi}{\partial y}+\frac{\partial\psi}{\partial x}\right) \end{bmatrix} - B\begin{bmatrix} \frac{\partial^2 w}{\partial x^2}+\upsilon\frac{\partial^2 w}{\partial y^2} \\ \frac{\partial^2 w}{\partial y^2}+\upsilon\frac{\partial^2 w}{\partial x^2} \\ (1-\upsilon)\frac{\partial^2 w}{\partial x\partial y} \end{bmatrix} + G\begin{bmatrix} \frac{\partial u_0}{\partial x}+\upsilon\frac{\partial v_0}{\partial y} \\ \frac{\partial v_0}{\partial y}+\upsilon\frac{\partial u_0}{\partial x} \\ \frac{1-\upsilon}{2}\left(\frac{\partial u_0}{\partial y}+\frac{\partial v_0}{\partial x}\right) \end{bmatrix} \quad (22b)$$

$$\begin{bmatrix} N_{xx} \\ N_{yy} \\ N_{xy} \end{bmatrix} = C\begin{bmatrix} \frac{\partial\phi}{\partial x}+\upsilon\frac{\partial\psi}{\partial y} \\ \frac{\partial\psi}{\partial y}+\upsilon\frac{\partial\phi}{\partial x} \\ \frac{1-\upsilon}{2}\left(\frac{\partial\phi}{\partial y}+\frac{\partial\psi}{\partial x}\right) \end{bmatrix} - G\begin{bmatrix} \frac{\partial^2 w}{\partial x^2}+\upsilon\frac{\partial^2 w}{\partial y^2} \\ \frac{\partial^2 w}{\partial y^2}+\upsilon\frac{\partial^2 w}{\partial x^2} \\ (1-\upsilon)\frac{\partial^2 w}{\partial x\partial y} \end{bmatrix} + S\begin{bmatrix} \frac{\partial u_0}{\partial x}+\upsilon\frac{\partial v_0}{\partial y} \\ \frac{\partial v_0}{\partial y}+\upsilon\frac{\partial u_0}{\partial x} \\ \frac{1-\upsilon}{2}\left(\frac{\partial u_0}{\partial y}+\frac{\partial v_0}{\partial x}\right) \end{bmatrix} \quad (22c)$$

$$\begin{Bmatrix} Q_x \\ Q_y \end{Bmatrix} = F\begin{Bmatrix} \phi \\ \psi \end{Bmatrix}, \quad (22d)$$

where

$$(S,G,B)=\int_{-\frac{h}{2}}^{\frac{h}{2}}\frac{E(Z)}{1-\upsilon^2}\left(1,z,z^2\right)zdz\,, \quad (23a)$$

$$(A,C,D)= \quad (23b)$$

$$\int_{-\frac{h}{2}}^{\frac{h}{2}}\frac{E}{1-\upsilon^2}(zf(z),f(z),(f(z))^2)dz,$$

$$(F)=\int_{-\frac{h}{2}}^{\frac{h}{2}}\frac{E(z)}{2(1+\upsilon)}\left(\frac{df(z)}{dz}\right)^2 dz, \quad (23c)$$

Substituting Eqs. (22a)–(22d) into Eqs. (19a)–(19e), yields to the following equations:

$$\frac{(1-\upsilon)}{2}\left(S\left(\frac{\partial^2 u_0}{\partial y^2}+\frac{\partial^2 v_0}{\partial x\partial y}\right)+C\left(\frac{\partial^2\phi}{\partial y^2}+\frac{\partial^2\psi}{\partial x\partial y}\right)-2G\frac{\partial^3 w}{\partial x\partial y^2}\right)+S\left(\frac{\partial^2 u_0}{\partial x^2}+\upsilon\frac{\partial^2 v_0}{\partial x\partial y}\right)+C\left(\frac{\partial^2\phi}{\partial x^2}+\upsilon\frac{\partial^2\psi}{\partial x\partial y}\right)-G\left(\frac{\partial^3 w}{\partial x^3}+\upsilon\frac{\partial^3 w}{\partial y^3}\right)=I_0\frac{\partial^2 u_0}{\partial t^2}$$

$$-I_1\frac{\partial^3 w}{\partial x\partial t^2}+I_3\frac{\partial^2\phi}{\partial t^2}-\mu^2\left(I_0\frac{\partial^4 u_0}{\partial t^2\partial x^2}-I_1\frac{\partial^5 w}{\partial x\partial t^2\partial x^2}+I_3\frac{\partial^4\phi}{\partial t^2\partial x^2}+I_0\frac{\partial^4 v_0}{\partial t^2\partial y^2}-I_1\frac{\partial^5 w}{\partial y\partial t^2\partial y^2}+I_3\frac{\partial^4\phi}{\partial t^2\partial y^2}\right) \quad (24a)$$

$$S\left(\frac{\partial^2 v_0}{\partial y^2}+\upsilon\frac{\partial^2 u_0}{\partial x\partial y}\right)+C\left(\frac{\partial^2 \psi}{\partial y^2}+\upsilon\frac{\partial^2 \phi}{\partial x\partial y}\right)+$$
$$\frac{(1-\upsilon)}{2}\left(S\left(\frac{\partial^2 u_0}{\partial x\partial y}+\frac{\partial^2 v_0}{\partial y^2}\right)+C\left(\frac{\partial^2 \phi}{\partial x\partial y}+\frac{\partial^2 \psi}{\partial x^2}\right)-\right.$$
$$\left.2G\frac{\partial^3 w}{\partial x^2\partial y}\right)-G\left(\frac{\partial^3 w}{\partial y^3}+\upsilon\frac{\partial^3 w}{\partial x^2\partial y}\right)=I_0\frac{\partial^2 v_0}{\partial t^2}$$
$$-I_1\frac{\partial^3 w}{\partial y\partial t^2}+I_3\frac{\partial^2 \psi}{\partial t^2}-\mu^2\left(I_0\frac{\partial^4 v_0}{\partial t^2\partial x^2}-I_1\frac{\partial^5 w}{\partial y\partial t^2\partial y^2}\right.$$
$$\left.+I_3\frac{\partial^4 \psi}{\partial t^2\partial x^2}+I_0\frac{\partial^4 v_0}{\partial t^2\partial y^2}-I_1\frac{\partial^5 w}{\partial y\partial t^2\partial y^2}+I_3\frac{\partial^4 \psi}{\partial t^2\partial y^2}\right) \quad (24b)$$

$$G\left(\frac{\partial^3 v_0}{\partial y^3}+\upsilon\frac{\partial^3 u_0}{\partial x\partial y^2}\right)+A\left(\frac{\partial^3 \psi}{\partial y^3}+\upsilon\frac{\partial^3 \phi}{\partial x\partial y^2}\right)+$$
$$(1-\upsilon)\left(G\left(\frac{\partial^3 u_0}{\partial x\partial y^2}+\frac{\partial^3 v_0}{\partial x^2\partial y}\right)\right)+A\left(\frac{\partial^3 \psi}{\partial x^2\partial y}+\right.$$
$$\left.\frac{\partial^3 \phi}{\partial x\partial y^2}\right)-2B\frac{\partial^4 w}{\partial x^2\partial y^2}\Big)-A\left(\frac{\partial^4 w}{\partial y^4}+\upsilon\frac{\partial^4 w}{\partial x^2\partial y^2}\right)$$
$$+G\left(\frac{\partial^3 u_0}{\partial x^3}+\upsilon\frac{\partial^3 v_0}{\partial x^2\partial y}\right)+A\left(\frac{\partial^3 \phi}{\partial x^3}+\upsilon\frac{\partial^3 \psi}{\partial x^2\partial y}\right)$$
$$-B\left(\frac{\partial^4 w}{\partial x^4}+\upsilon\frac{\partial^4 w}{\partial x^2\partial y^2}\right)=I_0\frac{\partial^2 w}{\partial t^2}+$$
$$I_1\left(\frac{\partial^3 u_0}{\partial x\partial t^2}+\frac{\partial^3 v_0}{\partial y\partial t^2}\right)-I_2\left(\frac{\partial^4 w}{\partial x^2\partial t^2}+\frac{\partial^4 w}{\partial y^2\partial t^2}\right)+$$
$$I_4\left(\frac{\partial^3 \phi}{\partial x\partial t^2}+\frac{\partial^3 \psi}{\partial y\partial t^2}\right)-\mu^2\left(I_0\frac{\partial^4 w}{\partial t^2\partial x^2}+\right.$$
$$I_1\left(\frac{\partial^5 u_0}{\partial x\partial t^2\partial x^2}+\frac{\partial^5 v_0}{\partial y\partial t^2\partial x^2}\right)$$
$$\left.-I_2\left(\frac{\partial^6 w}{\partial x^2\partial t^2\partial x^2}+\frac{\partial^6 w}{\partial y^2\partial t^2\partial x^2}\right)\right) \quad (24c)$$

$$\frac{(1-\upsilon)}{2}\left(C\left(\frac{\partial^2 u_0}{\partial y^2}+\frac{\partial^2 v_0}{\partial x\partial y}\right)+D\left(\frac{\partial^2 \phi}{\partial y^2}+\frac{\partial^2 \psi}{\partial x\partial y}\right)\right.$$
$$\left.-2A\frac{\partial^3 w}{\partial x\partial y^2}\right)+C\left(\frac{\partial^2 u_0}{\partial x^2}+\upsilon\frac{\partial^2 v_0}{\partial x\partial y}\right)+D\left(\frac{\partial^2 \phi}{\partial x^2}+\right.$$
$$\left.\upsilon\frac{\partial^2 \psi}{\partial x\partial y}\right)-A\left(\frac{\partial^3 w}{\partial x^3}+\upsilon\frac{\partial^3 w}{\partial x\partial y^2}\right)-F\phi=I_3\frac{\partial^2 u_0}{\partial t^2}$$
$$-I_4\frac{\partial^3 w}{\partial x\partial t^2}+I_5\frac{\partial^2 \phi}{\partial t^2}-\mu^2\left(I_3\frac{\partial^4 u_0}{\partial t^2\partial x^2}-I_4\frac{\partial^5 w}{\partial x\partial t^2\partial x^2}+\right.$$
$$I_5\frac{\partial^4 \phi}{\partial t^2\partial x^2}+I_3\frac{\partial^4 u_0}{\partial t^2\partial y^2}-I_4\frac{\partial^5 w}{\partial x\partial t^2\partial y^2}+$$
$$\left.I_5\frac{\partial^4 \phi}{\partial t^2\partial y^2}\right) \quad (24d)$$

$$C\left(\frac{\partial^2 v_0}{\partial y^2}+\upsilon\frac{\partial^2 u_0}{\partial x\partial y}\right)+D\left(\frac{\partial^2 \psi}{\partial y^2}+\upsilon\frac{\partial^2 \phi}{\partial x\partial y}\right)+$$
$$+\frac{(1-\upsilon)}{2}\left(C\left(\frac{\partial^2 u_0}{\partial x\partial y}+\frac{\partial^2 v_0}{\partial x^2}\right)+D\left(\frac{\partial^2 \phi}{\partial x\partial y}+\frac{\partial^2 \psi}{\partial x^2}\right)\right.$$
$$\left.-2A\frac{\partial^3 w}{\partial x^2\partial y}\right)-A\left(\frac{\partial^3 w}{\partial y^3}+\upsilon\frac{\partial^3 w}{\partial x^2\partial y}\right)-H\psi=$$
$$I_3\frac{\partial^2 v_0}{\partial t^2}-I_4\frac{\partial^3 w}{\partial y\partial t^2}+$$
$$I_5\frac{\partial^2 \psi}{\partial t^2}-\mu^2\left(I_3\frac{\partial^4 v_0}{\partial t^2\partial x^2}-I_4\frac{\partial^5 w}{\partial y\partial t^2\partial x^2}+\right.$$
$$I_5\frac{\partial^4 \psi}{\partial t^2\partial x^2}+I_3\frac{\partial^4 v_0}{\partial t^2\partial y^2}-I_4\frac{\partial^5 w}{\partial y\partial t^2\partial y^2}+$$
$$\left.I_5\frac{\partial^4 \psi}{\partial t^2\partial y^2}\right) \quad (24e)$$

It can be seen that Eqs. (24a)-(24e) are coupled functions of displacements. The permissible displacement and rotation functions that can be satisfied with the simply supported boundary conditions at all edges of the plate are trigonometric series. Using Navier's solution, the explanation of the displacement and rotations is as what follows:

$$u_0=\sum_{m=1}^{\infty}\sum_{n=1}^{\infty}u_{mn}\cos(\gamma x)\sin(\beta y)\sin(\lambda_{mn}t) \quad (25a)$$

$$v_0=\sum_{m=1}^{\infty}\sum_{n=1}^{\infty}v_{mn}\sin(\gamma x)\cos(\beta y)\sin(\lambda_{mn}t) \quad (25b)$$

$$w=\sum_{m=1}^{\infty}\sum_{n=1}^{\infty}W_{mn}\sin(\gamma x)\sin(\beta y)\sin(\lambda_{mn}t) \quad (25c)$$

$$\phi=\sum_{m=1}^{\infty}\sum_{n=1}^{\infty}\Phi_{mn}\cos(\gamma x)\sin(\beta y)\sin(\lambda_{mn}t) \quad (25d)$$

$$\psi=\sum_{m=1}^{\infty}\sum_{n=1}^{\infty}\Psi_{mn}\sin(\gamma x)\cos(\beta y)\sin(\lambda_{mn}t) \quad (25e)$$

Where $\gamma=n\pi/a$ and $\beta=m\pi/b$ are the numbers of half wave correlation to x and y directions. u_{mn}, $v_{mn}$and W_{mn} are the amplitudes of translation and Φ_{mn} and $\Psi_{mn}$are the amplitudes of rotations. λ_{mn} is the frequency of the linear free vibration. a is the width of the edge and b is the length of the edge. Substituting Eqs. (25a)-(25e) into Eqs. (24a)-(24e)yields to what follows:

$$([K]-\lambda_{mn}[M])\{\Delta\}=\{0\}, \quad (26)$$

The requisite for answering equation (26) except the obvious answer is that the determinant of coefficients matrix must be zero. Using this principle can be derived the characteristic equation.

3. Numerical example

Since the results of nanoplate made of FGM are not available in the open literature, to validate the results, in this paper have used two separate parts;in the first part, have been validated Isotropic rectangular nanoplate, and in the second part, it does for FGM one.

3.1. Isotropic rectangular nanoplate

Only homogeneous plate ($g = 0$) is used herein for the verification. Tables 2-4 list the first three non-dimensional frequency and Frequency Ratios (FR) for simply supported boundary condition with various values of aspect ratio ($\eta = b / a$), specified values of non-dimensional nonlocal parameter ($\zeta = \mu / a$) and the thickness to lenghth ratio $h / a = 0.1$ on rectangular nanoplates. The natural frequency parameters expressed in dimensionless form $\beta = a\omega^2\sqrt{\rho h / D}$, $D = Eh^3 / 12(1-\nu^2)$ are the flexural rigidity. The nanoplate is made of the following material properties: $E = 210Gpa$, $\upsilon = 0.3$ and $\rho = 7800$ (kg / m^3). The calculated frequencies based on the nonlocal exponential shear deformation theory are compared with those reported by Hosseini-Hashemi et al. [40] based on Mindlin Plate Theory (MPT). Also, the Frequency Ratio (FR) relation between the nonlocal and local dimensionless frequencies is expressed as what follows:

$$FR = \frac{\beta^{NL}}{\beta^{L}} \tag{27}$$

where β^{NL} is the non-dimensianal nonlocal frequency parameter, and β^{L} is the non-dimensional local frequency parameter.

Table 2. The variations of the non-dimensional frequency ($\beta = a\omega^2\sqrt{\rho h / D}$) and the frequency ratio (FR) for the nonlocal plate(*m*=1, *n*=1)

	Method		ζ =0	ζ =0.2	ζ =0.4	ζ =0.6	ζ =0.8
		β^{NL}	FR	FR	FR	FR	FR
$\eta = 0.6$	Present	35.015	1.0000	0.6335	0.3789	0.2633	0.2005
	Exact [40]	35.0643	1.0000	0.6335	0.3789	0.2633	0.2005
$\eta = 0.8$	Present	24.2084	1.0000	0.7051	0.4451	0.1346	0.2412
	Exact [40]	24.2330	1.0000	0.7050	0.4451	0.3146	0.2412
$\eta = 1$	Present	19.0684	1.0000	0.7475	0.4904	0.3512	0.2708
	Exact [40]	19.0840	1.0000	0.7475	0.4904	0.3512	0.2708

Table 3. The variations of the non-dimensional frequency ($\beta = a\omega^2\sqrt{\rho h / D}$) and the frequency ratio (FR) for the nonlocal plate(*m*=2, *n*=1)

	Method		ζ =0	ζ =0.2	ζ =0.4	ζ =0.6	ζ =0.8
		β^{NL}	FR	FR	FR	FR	FR
$\eta = 0.6$	Present	60.1556	1.0000	0.5216	0.2923	0.1997	0.1511
	Exact [40]	60.2869	1.0000	0.5216	0.2923	0.1997	0.1511
$\eta = 0.8$	Present	50.2147	1.0000	0.5594	0.3197	0.2194	0.1663
	Exact [40]	50.3100	1.0000	0.5594	0.3197	0.2194	0.1664
$\eta = 1$	Present	45.5048	1.0000	0.5799	0.3353	0.2308	0.1752
	Exact [40]	45.5845	1.0000	0.5799	0.3353	0.2308	0.1752

Table 4. The variations of the non-dimensional frequency ($\beta = a\omega^2\sqrt{\rho h / D}$) and the frequency ratio (FR) for the nonlocal plate(*m*=2, *n*=2)

	Method		ζ =0	ζ =0.2	ζ =0.4	ζ =0.6	ζ =0.8
		β^{NL}	FR	FR	FR	FR	FR
$\eta = 0.6$	Present	121.356	1.0000	0.3789	0.2005	0.1352	0.1018
	Exact [40]	121.7700	1.0000	0.3789	0.2006	0.1352	0.1018
$\eta = 0.8$	Present	86.9898	1.0000	0.4451	0.2412	0.1635	0.1233
	Exact [40]	87.2357	1.0000	0.4451	0.2412	0.1635	0.1233
$\eta = 1$	Present	69.8517	1.0000	0.4904	0.2708	0.1843	0.1393
	Exact [40]	70.0219	1.0000	0.4904	0.2708	0.1844	0.1393

According to the Eqs. (1) and (2),when the power law index g approaches zero or infinity,the plate is isotropic composed of fully ceramic or metal, respectively.Three fundamental frequency parameters β of SSSS AL / AL_2o_3 square plate ($\eta = 1$) are presented in Table 5 for $\delta = 0.1$and 0.2.The results are compared with those obtained by Shufrin and Eisenberger[45] based on the HSDT. It is found that when gradient index approaches zero or infinity the frequency parameters of FG plate converge to relevant isotropic one. The excellent agreement among the reults confirms the high accuracy of the current analytical approach.

3.2. FGM square plate

Table 6 shows a comparison of the frequency parameters $\widehat{\beta} = \omega h\sqrt{\rho_c / E_c}$ for AL / AL_2o_3 square moderately thick plates with those obtained by Hosseini-Hashemi et al. [46], Zhao et al. [47] and Masunaga [32] when $g = 0$, 0.5, 1, 4 and 10. In addition, the corresponding mode shapes m and n, denoting the number of half-waves in the x and y directions, respectively, are present for any of the frequency parameters $\widehat{\beta}$. Also, in Table 7,a comparison of the frequency parameters $\bar{\beta} = \omega h\sqrt{\rho_m / E_m}$ for a simply supported AL / ZrO_2 square plates with those of two-dimensional higher-order theory [32], three-dimensional theory by employing the power series method [48], finite element HSDT method [49], finite element FSDT method[49] and an analytical FSDT solution [46] is shown. From Tables 6 and 7, it is evident that there is a very good agreement among the results confirming the high accuracy of the current analytical approach.

Table 5. The comparison of the fundamental frequency parameters ($\beta = \omega a^2\sqrt{\rho_c / E_c} / h$) for AL / AL_2o_3 square plates ($\eta = 1$)

Material	Method	g	h / a	
			0.1	0.2
Fully ceramic	Present	10^{-3}	5.7681	5.2826
		10^{-4}	5.7701	5.2843
		10^{-5}	5.7703	5.2845
		10^{-6}	5.7703	5.2845
	HSDT[45]	0	5.7694	5.2813
Fully metallic	Present	10^{2}	2.8235	2.8235
		10^{3}	2.7051	2.7051
		10^{4}	2.9389	2.6913
		10^{5}	2.9372	2.6900
	HSDT[45]	∞	2.9376	2.6891

As it is seen, the present solution reports a good agreement with those obtained by the HSDT [32]for the thicker FG square plates ($\delta = 0.1, 0.2, 1/\sqrt{10}$) particularly at the higher modes of vibration. The difference between the present natural frequencies from those obtained by the 3-D method [48] may be due to the estimation of the material properties at a point where expressed by the local volume fractions and the material properties of the phases using two methods: Mori-Tanaka [50, 51]and the self-consistent scheme [52], whereas, in the present analysis, Material properties of the FGM layer are assumed to vary in the thickness direction according to a power law distribution. The difference between the present solutions from those obtained by the analytical FSDT solutions [46] is caused by vanishing of the in-plane displacement components of FG plate in Ref [46]. In fact, as the present procedure provided, the in-plane displacement components u and v should be taken into account and are coupled with the transverse displacement components w, ϕ , ψ and *m* and *n* are wave numbers in directions *x* and *y*, respectively.

4. Results and discussion

The vibration modes of FG plate may be divided into two main categories: the out-of-plane (transverese) modes and the in-plane modes. For the in-plane modes, the magnitude of the transverse displacement is very smaller than the magnitude of the in-plane displacements, u and v. There is a main difference between in-plane modes of isotropic plates and FG ones. When an isotropic plate has in-plane mode, there is no transverse displacement and the plate can only move along the in-plane directions but due to the existing coupling between in-plane and out-of-plane vibration in FG plate, in-plane mode includes two kinds of motion whereas in-plane vibration is dominant. InTabel 8, based on the present navier solutions and finite element method, the numerical results have been performed for Al / Al_2O_3 square plates ($\eta = 1$) when p=1. The lenghth of square plates is 1 m. Three different thicknesses 0.05 m (corresponding to thin plates), 0.1 m and 0.2 m (corresponding to moderately thick plate) and 0.3 m (corresponding to thick plates) have been used. All of the calculations are obtained for the first four natural frequencies.

The percentage difference given in Table 8 is defined as what follows:

$$\%Diff = \frac{|FEM - Navier|}{FEM} \times 100$$

Table 6. The comparison of the natural frequency parameter ($\hat{\beta} = \omega h\sqrt{\rho_c / E_c}$) for AL / AL_2o_3 square plates ($\eta = 1$)

h / a	(m,n)	Method	G				
			0	0.5	1	4	10
0.05	(1,1)	Present	0.0148	0.0125	0.0113	0.0098	0.0094
		FSDT[46]	0.0148	0.0128	0.0115	0.0101	0.0096
		FSDT[47]	0.0146	0.0124	0.0112	0.0097	0.0093
0.1	(1,1)	Present	0.0577	0.0490	0.0442	0.0381	0.0364
		HSDT[32]	0.0577	0.0492	0.0443	0.0381	0.0364
		FSDT[46]	0.0577	0.0492	0.0445	0.0383	0.0363
		FSDT[47]	0.0568	0.0482	0.0435	0.0376	0.3592
	(1,2)	Present	0.1377	0.1174	0.1059	0.0902	0.0856
		HSDT[32]	0.1381	0.1180	0.1063	0.0904	0.0859
		FSDT[47]	0.1354	0.1154	0.1042	-	0.085
	(2,2)	Present	0.2114	0.1808	0.1632	0.1377	0.1300
		HSDT[32]	0.2121	0.1819	0.1640	0.1383	0.1306
		FSDT[47]	0.2063	0.1764	0.1594	-	0.1289
0.2	(1,1)	Present	0.2114	0.1808	0.1632	0.1377	0.1300
		HSDT[32]	0.2121	0.1819	0.1640	0.1383	0.1306
		FSDT[46]	0.2112	0.1806	0.1650	0.1371	0.1304
		FSDT[47]	0.2055	0.1757	0.1587	0.1356	0.1284
	(1,2)	Present	0.4629	0.3993	0.3611	0.2976	0.2772
		HSDT[32]	0.4658	0.4040	0.3644	0.3000	0.2790
	(2,2)	Present	0.6691	0.5807	0.5254	0.4280	0.3947
		HSDT[32]	0.6753	0.5891	0.5444	0.4362	0.3981

Table 7. The comparison of the fundamental frequency parameter ($\hat{\beta} = \omega h\sqrt{\rho_m / E_m}$) for AL / ZrO_2 square plates ($\eta = 1$)

Method	g=0		g=1			$\delta = 0.2$		
	$\delta = \frac{1}{\sqrt{10}}$	$\delta = 0.1$	$\delta = 0.05$	$\delta = 0.1$	$\delta = 0.2$	g=2	g=3	g=5
Present	0.4629	0.0577	0.0158	0.0619	0.2278	0.2288	0.2301	0.2327
HSDT[32]	0.4658	0.0577	0.0158	0.0619	0.2285	0.2264	0.2270	0.2281
3-D[48]	0.4658	0.0577	0.0153	0.0596	0.2192	0.2197	0.2211	0.2225
HSDT[49]	0.4658	0.0578	0.0157	0.0613	0.2257	0.2237	0.2243	0.2253
FSDT[49]	0.4619	0.0577	0.0162	0.0633	0.2323	0.2325	0.2334	0.2334
FSDT[46]	0.4618	0.0576	0.0158	0.0611	0.2270	0.2249	0.2254	0.2265

An excellent agreement is observed between the present Navier solution and the FEM. The frequencies rise with an increase in the thickness of the plate due to an increase in the stiffiness of the plate. This phenomenon originates from increasing the rigidity of the plate. Although it is observed that the present solution can be predicts the in-plane modes of the plate. From the results are presented in this study one can be find that the natural frequencies are increased by increasing the thickness of the plate. This feature is due to the fact that the strain energy of the plate has significant sensibility with respect to the thickness. It is to be reminded that the out-of-plane modes depend on the bending energy, directly. Then, the number of the out-of-plane modes is increased. The influence of the aspect ratio $\eta = a / b$ on the frequency parameters β of a rectangular Al / ZrO_2 plate ($\delta = 0.2$, g=1) is shown in Table 9. From Table 9, it can be inferred that with a decrease in the aspect ratio, the frequency parameter increases, whereas the plate considering here is assumed to be simply supported in all edges, with decrease in length in a constant width, the degree of freedom (DOF) of the plate decreases, and it causes to increase the stiffness and the frequency parameter. In Table 10, the effects of different parameters

on the non-dimensional frequencies of the rectangular FG nanoplate are shown.From this Table, it is found that by increasing the nonlocal parameter, the rate of variation of non-dimensional frequencies decreases, because by increasing the nonlocal parameter, the strain energy decreases, and it causes a decrease in the plates rigidity. In Fig. 3, the effects of the aspect ratio and the nonlocal parameter on the nondimensional frequancy of the rectangular nanoplates are shown. It is shown that with an increase in the aspect ratio, the nondimensional frequancy increases.

Table 8. The first four natural frequency (Hz) for Al / Al_2O_3 square plates ($\eta = 1$, g=1)

$\frac{h}{a}$	Method	Mode			
		1	2	3	4
0.05	Present	359.92	889.33	1406.9	1745.7
	FEM[53]	357.37	883.58	1398.6	1736.2
	Diff(%)	0.7130	0.6500	0.5930	0.5470
0.1	Present	703.44	1686.0	2597.5	2597.5
	FEM[53]	699.30	1679.7	2578.7	2592.5
	Diff(%)	0.5920	0.3750	0.7290	0.1930
0.2	Present	1298.8	2575.5	2873.5	3635.2
	FEM[53]	1296.3	2574.6	2883.0	3633.3
	Diff(%)	0.1930	0.0350	0.3230	0.0520
0.3	Present	1755.2	2569.7	3618.8	3607.4
	FEM[53]	1759.8	2567.7	3613.3	3613.3
	Diff(%)	0.2610	0.0780	0.1520	0.1630

Table 9. The frequency parameter ($\hat{\beta} = \omega a^2 \sqrt{\rho_c / E_c} / h$) for AL / ZrO_2 square plates ($\delta = 0.2$, g=1)

$\frac{a}{b}$	2	1.5	1	2/3	0.5
Mode	3.1198	3.3720	4.9325	6.9551	9.9853

Table 10. The effect of the non-dimensional nonlocal parameter ζ and the power law index g on the non-dimensional frequencies of the rectangular FG nanoplate

ζ	$\frac{a}{b}$	$\frac{h}{a}$	Power low index		
			0	5	10
0.0	0.5	0.2	0.2114	0.1357	0.0856
		0.1	0.0365	0.0239	0.0231
	1.0	0.2	0.2310	0.1356	0.1300
		0.1	0.0577	0.0377	0.0364
0.1	0.5	0.2	0.1299	0.1239	0.0808
		0.1	0.0345	0.0226	0.0218
	1.0	0.2	0.1932	0.1239	0.1188
		0.1	0.0527	0.0344	0.0332
0.2	0.5	0.2	0.1127	0.0728	0.0700
		0.1	0.0299	0.0196	0.0189
	1.0	0.2	0.1580	0.1014	0.0972
		0.1	0.0431	0.0282	0.0272
0.3	0.5	0.2	0.0948	0.0613	0.0589
		0.1	0.0251	0.0165	0.0159
	1.0	0.2	0.1269	0.0814	0.0780
		0.1	0.0346	0.0226	0.0218
0.4	0.5	0.2	0.0798	0.0516	0.0496
		0.1	0.0212	0.0139	0.0134
	1.0	0.2	0.1037	0.0665	0.0638
		0.1	0.0283	0.0185	0.0178

It is illustrated that for the lower aspect ratios, the influence of the nonlocal parameters decreases. Also in Fig. 4, the effects of the aspect ratio and the nonlocal parameter on the frequancy ratio of the rectangular nanoplates are shown for different modes of vibration. From this figure, it seems that the frequancy ratios for the lower modes are more than those for the upper modes.

From Fig. 5, it is found that for lowerpower low index, the rate of The nondimensional frequencies are higher,and The effect of non-dimensional nonlocal parameter on The non-dimensional frequencies are significant, and diminishes with increase in that.Because by increase in the power low index, property of plate approaches to metal, and it's stiffness decreases, thus itcauses to decrease non-dimentionalfrequencuy.

From this figure, it is shown that in investigating the FG nanoplates, the effects of nonlocal parameter cannot be ignored so the theories for macro plates arenot suitable for nanoplates.

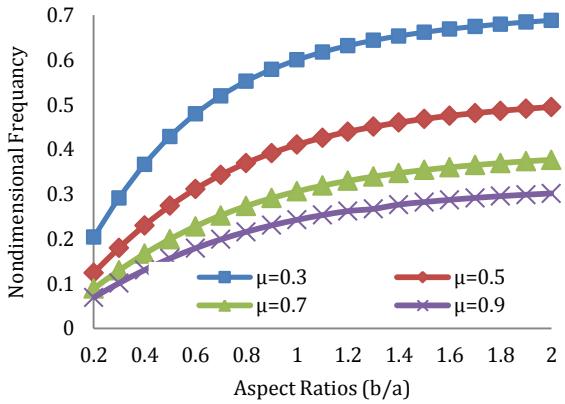

Figure 3. The effects of the aspect ratio and the nonlocal parameter on the nondimensional frequancy

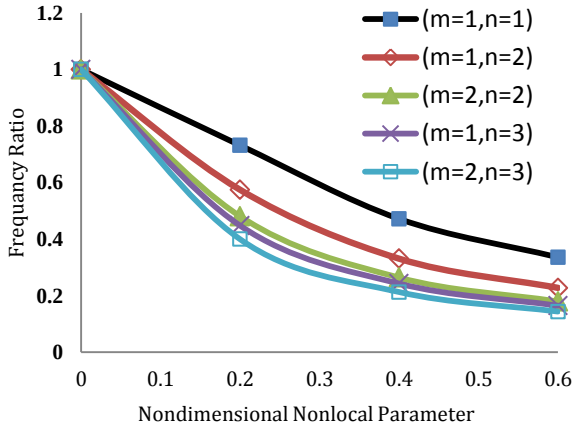

Figure 4. The effects of the aspect ratio and the nonlocal parameter on the nondimensional frequancy

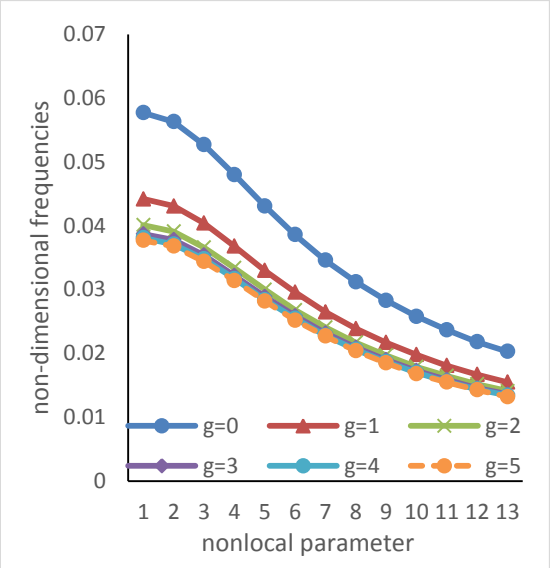

Figure 5. The effects of the nonlocal parameter μ and the power law index on the non-dimensional frequency of the square nanoplate (mode (1,1), $h/a=0.1$)

5. Conclusion

A Navier method was applied to the free vibration of the functionally graded rectangular nanoplates. The formulations were based on the exponential shear deformation theory using the nonlocal elasticity theory, and Hamilton's principle was used to derive the equations of motion and associated boundary conditions. Comparing the cases with those reported in the literature for simply supported rectangular FG nano-plates demonstrates a high stability and accuracy of the present solution. What presented herein shows the effects of the variations of the nonlocal parameter, the ratio of the thickness to the length, the power law indexes and the aspect ratio on the frequency values of a FG nano-plate. It's shown that the frequency ratio decreases with increasing the mode number and the value of the nonlocal parameter, and also increasing the power law index causes the non-dimensional frequencies to decrease. All analytical results presented here can provide other research groups with a reliable source to check out their analytical and numerical solutions.

References

[1] Iijima S. Helical microtubules of graphitic carbon. *nature* 1991; 354: 56-58.

[2] Miller RE, Shenoy VB. Size-dependent elastic properties of nanosized structural elements. *Nanotechnology* 2000; 11: 139.

[3] Shen HS. Zhang CL. Torsional buckling and postbuckling of double-walled carbon nanotubes by nonlocal shear deformable shell model. *Compos Struct* 2010; 92: 1073-1084.

[4] Aydogdu M. Axial vibration of the nanorods with the nonlocal continuum rod model. *Phys E* 2009; 41: 861-864.

[5] Wang CM, Duan W. Free vibration of nanorings/arches based on nonlocal elasticity. *Appl Phys* 2008; 104: 014303.

[6] Pradhan S, Phadikar J. Small scale effect on vibration of embedded multilayered graphene sheets based on nonlocal continuum models. *Phys Lett A* 2009; 373: 1062-1069.

[7] Ma M, et al. Electrochemical performance of ZnO nanoplates as anode materials for Ni/Zn secondary batteries. *J Power Sources* 2008; 179: 395-400.

[8] Craighead HG. Nanoelectromechanical systems. *Sci* 2000; 290: 1532-1535.

[9] Sakhaee-Pour A, Ahmadian M, Vafai A. Applications of single-layered graphene sheets as mass sensors and atomistic dust detectors. *Solid State Commun* 2008; 145: 168-172.

[10] Sakhaee-Pour A, Ahmadian M, Vafai A. Potential application of single-layered graphene sheet as strain sensor. *Solid State Commun* 2008; 147: 336-340.

[11] Aagesen M. Sorensen C. Nanoplates and their suitability for use as solar cells. *Proceedings of Clean Technol* 2008; 109-112.

[12] Ye C, et al. Thickness-dependent photocatalytic performance of ZnO nanoplatelets. *J Phys Chem B* 2006; 110: 15146-15151.

[13] Rafiee MA, et al. Fracture and fatigue in graphene nanocomposites. *small* 2010; 6: 179-183.

[14] Kong S, et al. The size-dependent natural frequency of Bernoulli–Euler micro-beams. Int J Eng Sci 2008; 46: 427-437.

[15] Fleck N, Hutchinson J. Strain gradient plasticity. *Adv Appl Mech* 1997;33 :296-361.

[16] Yang F, et al. Couple stress based strain gradient theory for elasticity. *Int J Sol Struct* 2002; 39: 2731-2743.

[17] Eringen AC, Edelen D. On nonlocal elasticity. *Int J Eng Sci* 1972; 10: 233-248.

[18] Peddieson J, Buchanan GR, McNitt RP. Application of nonlocal continuum models to nanotechnology. *Int J Eng Sci* 2003; 41: 305-312.

[19] Reddy J. Nonlocal theories for bending, buckling and vibration of beams. *Int J Eng Sci* 2007; 45: 288-307.

[20] Reddy J. Pang S. Nonlocal continuum theories of beams for the analysis of carbon nanotubes. J App Phys 2008; 103: 023511.
[21] Heireche H, et al. Sound wave propagation in single-walled carbon nanotubes using nonlocal elasticity. *Phys E 2008*; 40: 2791-2799.
[22] Murmu T, Pradhan S. Buckling analysis of a single-walled carbon nanotube embedded in an elastic medium based on nonlocal elasticity and Timoshenko beam theory and using DQM. *Phys E* 2009; 41: 1232-1239.
[23] Murmu T, Pradhan S. Thermo-mechanical vibration of a single-walled carbon nanotube embedded in an elastic medium based on nonlocal elasticity theory. *Comput Mater Sci* 2009; 46: 854-859.
[24] Wang L. Dynamical behaviors of double-walled carbon nanotubes conveying fluid accounting for the role of small length scale. *Comput Mater Sci* 2009; 45: 584-588.
[25] Eringen AC. On differential equations of nonlocal elasticity and solutions of screw dislocation and surface waves. *J appl phys* 1983; 54: 4703-4710.
[26] Chen Y, Lee JD, Eskandarian A. Atomistic viewpoint of the applicability of microcontinuum theories. *Int j sol struct* 2004; 41: 2085-2097.
[27] Malekzadeh P, Heydarpour Y. Free vibration analysis of rotating functionally graded cylindrical shells in thermal environment. *Compos Struct* 2012; 94: 2971-2981.
[28] Ungbhakorn V, Wattanasakulpong N. Thermo-elastic vibration analysis of third-order shear deformable functionally graded plates with distributed patch mass under thermal environment. *Appl Acoust* 2013; 74: 1045-1059.
[29] Kumar Y, Lal R. Prediction of frequencies of free axisymmetric vibration of two-directional functionally graded annular plates on Winkler foundation. *Eur J Mech A Solid* 2013; 42: 219-228.
[30] Nie G, Zhong Z. Semi-analytical solution for three-dimensional vibration of functionally graded circular plates. *Comput Method Appl M* 2007; 196: 4901-4910.
[31] Huang C, Yang P, Chang M. Three-dimensional vibration analyses of functionally graded material rectangular plates with through internal cracks. *Compos Struct* 2012; 94: 2764-2776.
[32] Matsunaga H. Free vibration and stability of functionally graded plates according to a 2-D higher-order deformation theory. *Compos struct* 2008; 82: 499-512.
[33] Malekzadeh P, Beni AA. Free vibration of functionally graded arbitrary straight-sided quadrilateral plates in thermal environment. *Compos Struct* 2010; 92: 2758-2767.
[34] Ke L, et al. Axisymmetric nonlinear free vibration of size-dependent functionally graded annular microplates. *Compos Part B: Engineering* 2013; 53: 207-217.
[35] Ke LL, et al. Bending, buckling and vibration of size-dependent functionally graded annular microplates. *Compos struct* 2012; 94: 3250-3257.
[36] Asghari M, Taati E. A size-dependent model for functionally graded micro-plates for mechanical analyses. *J Vib Cont* 2013; 19: 1614-1632.
[37] Natarajan S, et al. Size-dependent free flexural vibration behavior of functionally graded nanoplates. *Comput Mater Sci* 2012; 65: 74-80.
[38] Thai HT, Choi DH. Size-dependent functionally graded Kirchhoff and Mindlin plate models based on a modified couple stress theory. *Compos Struct* 2013; 95: 142-153.
[39] Reddy J. Microstructure-dependent couple stress theories of functionally graded beams. *J Mech Phys of Solids* 2011; 59: 2382-2399.
[40] Hosseini-Hashemi S, Zare M, Nazemnezhad R. An exact analytical approach for free vibration of Mindlin rectangular nano-plates via nonlocal elasticity. *Compos Struct* 2013; 100: 290-299.
[41] Sahoo R, Singh B. A new trigonometric zigzag theory for static analysis of laminated composite and sandwich plates. *Aerosp sci technol* 2014; 35: 15-28.
[42] Narendar S. Buckling analysis of micro-/nano-scale plates based on two-variable refined plate theory incorporating nonlocal scale effects. *Compos Struct* 2011; 93: 3093-3103.
[43] Hosseini-Hashemi S, Bedroud M. Nazemnezhad R. An exact analytical solution for free vibration of functionally graded circular/annular Mindlin nanoplates via nonlocal elasticity. *Compos Struct* 2013; 103: 108-118.
[44] Sayyad AS, Ghugal YM. Bending and free vibration analysis of thick isotropic plates by using exponential shear deformation theory. *Appl Comput mech* 2012; 6: 1-12.

[45] Shufrin I, Eisenberger M. Stability and vibration of shear deformable plates––first order and higher order analyses. *Int j sol struc* 2005; 42: 1225-1251.

[46] Hosseini-Hashemi S, et al. Free vibration of functionally graded rectangular plates using first-order shear deformation plate theory. *Appl Math Model* 2010; 34: 1276-1291.

[47] Zhao X, Lee Y, Liew KM. Free vibration analysis of functionally graded plates using the element-free kp-Ritz method. *J sound Vibration* 2009; 319: 918-939.

[48] Vel SS, Batra R. Three-dimensional exact solution for the vibration of functionally graded rectangular plates. *J Sound Vibration* 2004; 272: 703-730.

[49] Pradyumna S, Bandyopadhyay J. Free vibration analysis of functionally graded curved panels using a higher-order finite element formulation. *J Sound Vibration* 2008; 318: 176-192.

[50] Mori T, Tanaka K. Average stress in matrix and average elastic energy of materials with misfitting inclusions. *Acta metallurgica* 1973; 21: 571-574.

[51] Benveniste Y. A new approach to the application of Mori-Tanaka's theory in composite materials. *Mech mater* 1987; 6: 147-157.

[52] Hill R. A self-consistent mechanics of composite materials. *J Mech Phys Sol* 1965; 13: 213-222.

[53] Hosseini-Hashemi S, Fadaee M, Atashipour SR. Study on the free vibration of thick functionally graded rectangular plates according to a new exact closed-form procedure. *Compos Struc* 2011; 93: 722-735.